Development of a Stable High-Temperature Diamond Thermistor Using Enhanced Supporting Designs

Tong J. Kim, Kurt L. Davis, Yunpeng Liu, John R. Bredemann, Zhenqiang Ma, *Fellow, IEEE*, Mark Anderson, and Michael L. Corradini

***Abstract*— Diamond is an excellent material for a high-temperature thermistor given its superior material properties. Despite its long history of the development, diamond thermistor is not widely used for commercial sensors because it is difficult to maintain optimum conditions for the diamond thermistor to operate at high temperature ranges in a compact size. In this paper, we demonstrate methods to improve the practicality and the feasibility of the diamond thermistor, focusing on the supporting components. The diamond thermistor design, where the diamond is sandwiched between contact pads, is tested up to 700 °C and being characterized by the Steinhart–Hart equations. For temperatures higher than 700 °C, the design of the thermistor is improved by encasing it in a metal sheath tube that protects and seals the diamond thermistor. Our supporting components provide oxygen free environment and a sturdy structure for the sensor components in a compact size. The encased diamond thermistor operates up to 880 °C and shows stable performance in a cycling test between 880 °C and the room temperature. An additional long-term stability test is performed at various temperatures for 10-hour durations. The tests show that the metal sheath tube design enables the diamond thermistor to be used as a practical temperature sensor at high-temperature ranges.**

***Index Terms*— CVD diamond, diamond thermistor, high temperature, laser welding, sheath tube.**

Manuscript received October 28, 2018; revised March 6, 2019; accepted March 8, 2019. Date of publication April 22, 2019; date of current version July 17, 2019. This work was supported by the Department of Energy (DOE): Advanced Instrumentation for Transient Reactor Testing under Grant DOE-NE0008305. The associate editor coordinating the review of this paper and approving it for publication was Dr. Ravibabu Mulaveesala. *(Corresponding author: Tong J. Kim.)*

T. J. Kim is with the National High Magnetic Field Laboratory, Tallahassee, FL 32310 USA (e-mail: tjkim@magnet.fsu.edu).

K. L. Davis is with the Idaho National Laboratory, Idaho Falls, ID 83415 USA (e-mail: kurt.davis@inl.gov).

Y. Liu was with the Engineering Physics Department, University of Wisconsin-Madison, Madison, WI 53705 USA. He is now with the Department of Nuclear Science and Engineering, Nanjing University of Aeronautics and Astronautics, Nanjing 210016, China (e-mail: liuyp@nuaa.edu.cn).

J. R. Bredemann was with the University of Wisconsin–Madison, Madison, WI 53705 USA. He is now with Epic Systems, Verona, WI 53593 USA (e-mail: jbredemann@wisc.edu).

Z. Ma is with the Electrical and Computer Engineering Department, University of Wisconsin–Madison, Madison, WI 53705 USA (e-mail: mazq@engr.wisc.edu).

M. Anderson is with the Mechanical Engineering Department, University of Wisconsin–Madison, Madison, WI 53705 USA (e-mail: manderson@engr.wisc.edu).

M. L. Corradini is with the Engineering Physics Department, University of Wisconsin–Madison, Madison, WI 53705 USA (e-mail: corradini@engr.wisc.edu).

Digital Object Identifier 10.1109/JSEN.2019.2912566

I. Introduction

A THERMISTOR is a device that measures the temperature by measuring its resistance. The resistance of a thermistor exhibits exponential decrement as temperature rises, due to the thermal excitations of carriers at a bandgap of the thermistor material [1], [2]. Diamond has been studied for its use as a thermistor since 1960 [3] because of its superior material properties such as extreme hardness [4]–[6], high thermal conductivity [7], [8], and a wide bandgap [9], [10]. The utmost hardness of the diamond prevents abrasion during the thermistor fabrication process, and the response time of the resistance from the surrounding temperature change is fast due to the high thermal conductivity [11]. The wide bandgap of diamond, 5.5 eV, produces less intrinsic carriers compared to other semiconductor materials as temperature increases, making the diamond thermistor to operate above several hundreds of degrees.

The diamond thermistor device is consisted of sensor components and supporting components. The sensor components are the diamond and ohmic contact pads where the temperature is detected. Early research on the diamond used natural diamonds with various types, each having a different concentration of the impurities [12]–[14]. In 1980s the synthetic diamonds were developed and widely used for industrial applications and research purposes due to the low manufacturing costs. Two methods were mainly used to synthesize diamond from the diamond seed. The first method was applying high temperature and high pressure (HPHT) to the diamond seed and the metal solvent that contains high purity carbon atoms. [15]–[18] The carbon atoms at the metal solvent start to grow at the diamond seed using the temperature gradient method under HPHT condition. The second method was using chemical vapor deposition (CVD) process that energize the hydrocarbon gas to grow the diamond in a film form on a substrate [19], [20]. The advantages of the CVD diamond are the control of the boron concentrations by varying the ratio of the gas mixture during the growth and selective growth on the substrate by using a sacrificial layer deposited with silicon oxides or silicon nitrides [21]–[24]. Combining these advantages led the expansion of thermistor development using CVD diamond films [25], [26]. The electrodes which are ohmic contact pads play a role in delivering electric signals from the diamond to the external measurement tool without energy barriers. Some metals are reported to be an

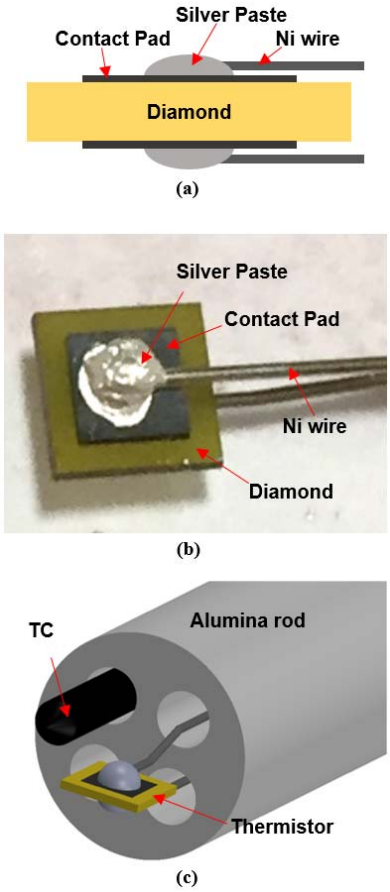

Fig. 1. Diamond thermistor with alumina rod. (a) Schematic of the basic diamond thermistor. (b) Image of HPHT diamond thermistor. (c) Schematic of the diamond thermistor and TC in the alumina rod.

ohmic contact with the diamond when annealed after the deposition by forming a carbide layer at the interface of the diamond [27]–[29].

The supporting components provide wire connections, mechanical support, and protection of the whole device from the extreme environment. The design and the materials for the supporting components need to be selected carefully because the sensor's stability, usability, and life-time are highly threatened as the measuring temperature increases. For example, when the supporting components do not provide oxygen free environment the diamond is attacked by the oxygen around 700 °C [30], [31] and ohmic contact layers lose their conduction as they are being oxidized [32], [33]. The mechanical stress is another problem because all the components have different thermal expansions that fail the electric connection to the diamond when the sensor is heated repeatedly. The importance of the supporting components is clear by reviewing the past works. The first diamond thermistor introduced by Rodgers and Raal [3] used Pt wires for the electrical connection to the natural diamond rod by directly welding with Ti-Ag-Cu alloy. The device was measured up to 350 °C showing the potential of diamond thermistor without the vacuum condition. Ran *et al.* [34] connected lead to the electrode of the diamond film thermistor. The device is measured up to 420 °C as the Si substrate begin to influence the resistance behavior. Yang *et al.* [35] clamped Tungsten probe with stainless steel on the electrode on the CVD diamond. The measurement was performed up to 950 K in an 18-inch stainless steel chamber to provide vacuum environment which is a quite large testing set-up. These past works did not show any results of repeatability of the sensor because the temperature is high enough to change the properties of the supporting components especially with the works without any vacuum condition. By compiling all the failing factors, the supporting components must maintain oxygen free environment in a compact size without disturbing the resistance of the diamond for the practical applications.

In this paper, we present a new design of the diamond thermistor and improved supporting components to enhance the practicality of the sensor. Our supporting components provide oxygen free environment and a sturdy structure to the sensor components in a compact size. The fabricated diamond thermistor is tested for repeatability and stability at high temperature ranges. Two types of commercially available synthesized diamonds (Element Six) were used for this work: a type-1b HPHT diamond and a boron-doped single crystal CVD diamond. The basic structure of our diamond thermistor without any reinforcing method was first verified with the operation of HPHT diamond thermistor at temperatures up to 700 °C. Then, issues regarding the wire connection to the diamond at high temperatures were raised, of which was improved by an introduction of a enhanced thermistor design with a metal sheath tube. Both the HPHT and CVD diamonds were fabricated in the improved design, and the operations of the thermistors were tested up to 850 °C and 880 °C, respectively. Additionally, the repeatability and stability of the CVD diamond thermistor with metal sheath tube were tested to prove the practicality of the new design.

II. Device Designs and Results

A. Diamond Thermistor With an Alumina Rod

The basic design of the diamond thermistor is shown in Fig. 1a. The diamond is sandwiched between two contact pads to measure the resistance through the diamond body. Metal wires were attached to the contact pad with silver paste to measure the resistance. The size of the HPHT and CVD diamonds are 3 mm by 3 mm with a thickness of 0.3 mm, and the orientation of the faces are {100}. In HPHT diamond, the doping concentration of boron is less than 0.1 ppm and 200 ppm for nitrogen. In the case of CVD diamond, the concentration of boron is less than 0.05 ppm and 1 ppm for the nitrogen.

On a side of HPHT diamond, the contact metal pad was patterned with photolithography and deposited with Mo and Pt (50 nm/ 150 nm) using an electron beam evaporator. A 2 mm by 2 mm contact pad remained at the center of the diamond after the lift-off process. Another contact pad was deposited using the same method at the opposite side of the diamond. To make the Ohmic contact between Mo and diamond, the diamond was placed in a vacuumed quartz tube and annealed in a furnace at 900 °C for 30 minutes. The Pt layer successfully prevented oxidation of Mo from the residual oxygen in the quartz tube during the annealing process, and the Mo/Pt pad showed the best stability at high temperature environment.

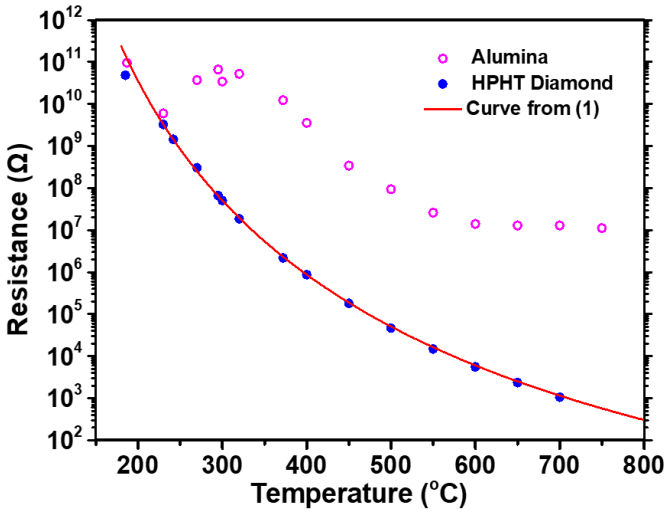

Fig. 2. The resistance measurement results of the HPHT diamond thermistor with the alumina tube design.

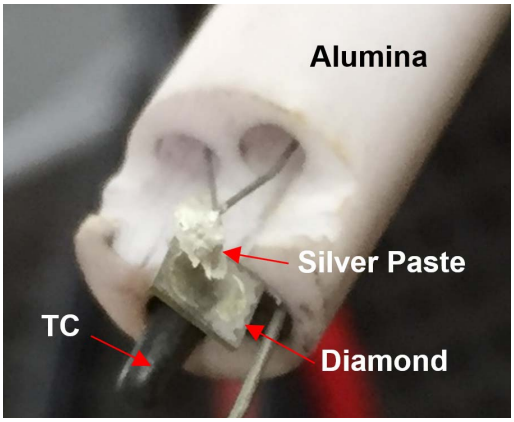

Fig. 3. The separation problem of silver paste detachment from the contact pad of the diamond after the resistance measurement test at 700 °C.

The surface of the diamond is not passivated because the thermistor is operating in the oxygen free environment.

The Ni wires were attached to the contact pads with two types of silver paste (597-A and 597-C, Aremco). The 597-C was first applied and cured between the contact pad and Ni wire since it showed better electrical conduction in a high temperature environment. The 597-A was applied and cured on top of 597-C to reinforce the adhesion strength. Fig. 1b shows a top view of the HPHT diamond thermistor after Ni wires were attached to the contact pads with two types of silver paste. Then, an alumina rod with four internal holes was employed to separate the Ni wires by threading the wires individually through the holes. For a reference temperature data, a thermocouple (TC, K-type, Omega) was inserted through a neighboring hole, and the measurement point of the TC was matched to the diamond thermistor region. Fig. 1c is a schematic image showing the diamond thermistor and the TC mounted in the alumina rod.

The wires were connected to the probes of the source-meter (Keithley 2602B) for the 2-wire measurement mode. The applied voltage was 1 V and the currents were measured to convert to resistance data. The resistance was measured after the furnace temperature was stabilized to a set temperature confirmed by reference temperature of the TC. Fig. 2 shows the resistance of the HPHT diamond thermistor with alumina tube design relative to the reference temperature of TC. The resistance data of the diamond as the temperature of the vacuum furnace increases from 150 °C up to 700 °C is plotted in blue dots. The test was repeated to measure the resistances of the alumina rod by removing the diamond thermistor and leaving only two Ni wires. The resistance data of the alumina rod is plotted in red circles in Fig. 2 to verify that there was no leakage of current through the alumina rod. The alumina rod effectively insulated the Ni wires since the resistance of the alumina rod was three orders higher than the resistance of the HPHT diamond throughout the test and the difference of the resistance became larger when the temperature exceeded 600 °C. Measuring the exact resistance over 5 GΩ was difficult because of the influence of the noise due to the low current level. This resulted in fluctuations of the resistance data around 10 GΩ. Thus, the exact resistance data was measured at 230 °C for the HPHT diamond and 400 °C for the alumina rod.

The resistance of the diamond can be converted into temperature data by the Steinhart-Hart equation which is a model for the resistance of semiconductors with reference to the temperatures [36]. The equation is:

$$\frac{1}{T} = A + Bln\,(R) + C[ln\,(R)]^3. \tag{1}$$

where T is temperature, R is the resistance of the semiconductor, and A, B, and C are Steinhart-Hart coefficients which can be calculated with 3 points of resistance data. Using the resistance data at 230 °C, 300 °C, and 400 °C, the calculated Steinhart-Hart coefficients for A, B, and C were 5.1457×10^{-4}, 7.3389×10^{-5}, and -1.2831×10^{-8}, respectively. With the extracted coefficients, a new resistance curve with respect to the temperature was calculated and drawn in the red line in Fig. 2. The measured diamond resistance data matched the calculated curve except at 185 °C because the exact resistance measurement was difficult due to the noise. Thus, any measured resistance data that is lower than 5 GΩ can be converted to temperature by matching it to the calculated resistance curve.

A problem with the alumina tube design was the detachment of silver paste from the contact pad on the diamond at a high temperature above 700 °C due to the thermal expansion differences between the diamond and the silver paste. Fig. 3 depicts this separation problem after the 700 °C measurement test. We noticed that the shape of the silver paste remained the same when it was first applied to the contact pads. Since the failure was not caused by the deformation of the silver paste, the improved design with the sheath tube was utilized to provide an additional clamping force to keep the wire connected to the diamond.

B. Diamond Thermistor With Metal Sheath Tube

A metal sheath tube was used to add a compression force to the diamond thermistor to maintain the electrical connection

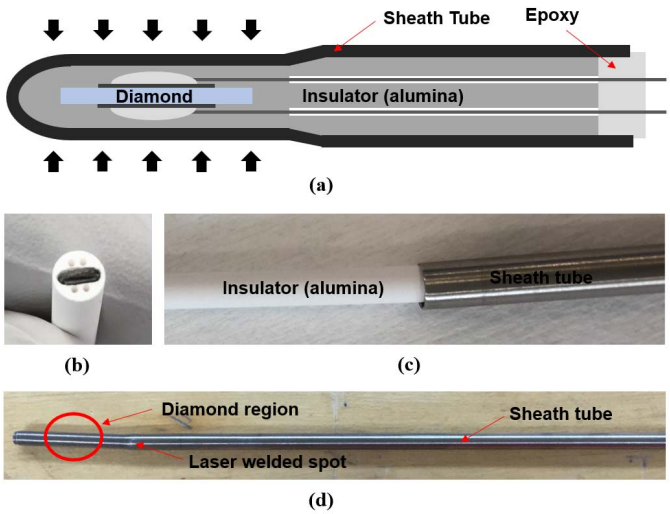

Fig. 4. Fabrication process of the diamond thermistor with sheath tube design. (a) Schematic of sheath tube design. (b) Diamond inserted in the CAR. (c) Inserting CAR into Sheath tube. (d) Complete diamond thermistor with the sheath tube.

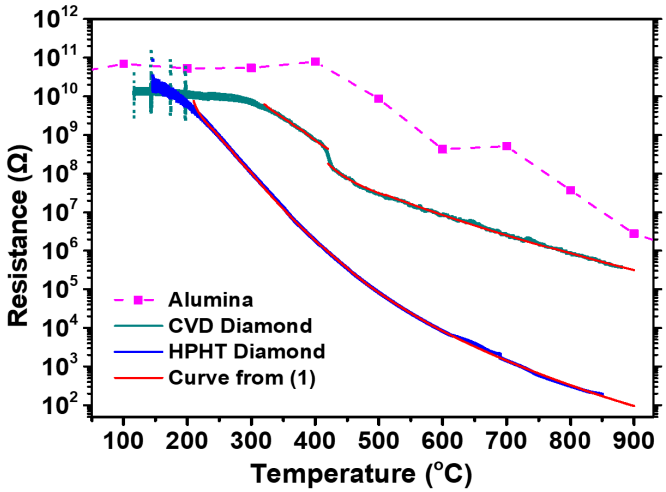

Fig. 5. The operation results of CVD and HPHT diamond thermistors fabricated with the metal sheath tube design.

in a high temperature environment. Fig. 4a is the schematic of the improved design with the metal sheath tube. The diamond thermistor components were encapsulated in a metal tube which provided a sturdy structural support and isolated the inside of the tube from the atmosphere. The material filling the inside of the metal tube was a crushable alumina rod (CAR) which is similar to chalk in terms of consistency and strength. It held the diamond thermistor and separated the wires for the resistance measurement. The front part of the metal tube where the diamond is located was compressed by a swaging process [37]. During the swaging process, the CAR fragmented into powder and tightened on the diamond thermistor to clamp the silver paste and the contact pads in place.

Fabrication of the diamond thermistor using the metal sheath tube design starts with inserting the diamond thermistor in the CAR. The CAR is 5 cm long with a diameter of 4.06 mm. It has holes for the wires to insert, and one end of the rod was drilled to fit the diamond. Fig. 4b shows the process by which the diamond thermistor was inserted in the CAR. The CAR was then inserted into the metal tube (Stainless Steel, 12 cm long) as in fig. 4c, followed by clamping both ends of the metal tube to prevent CAR from being pushed out during the swaging process. The outer diameter of the metal tube was reduced to 3.81 mm using the swaging machine (Torrington), which compressed the diamond thermistor as described above. After cutting the clamped region of the metal tube, the end without the wires was sealed with a stainless-steel plug by a laser welder (Laserstar). At the other end, the wires were threaded into CAR and inserted into the un-swaged metal tube as shown in Fig. 4c. The swaged and un-swaged metal tubes were welded together with a laser welder at the area shown in Fig. 4d. To remove oxygen inside the tube, a purging process was repeated several times by injecting high purity He gas into the metal tube with 1000 PSI and vacuuming to 0.1 mTorr. After the purging process, the assembly was soaked in a drying furnace for 12 hours and then sealed with epoxy to create the wire penetration.

Two types of diamond thermistors were fabricated with the metal sheath tube design using CVD and HPHT diamonds. The operation of the diamond thermistor was tested with a box furnace (Lindberg, 51442) without vacuum since the metal sheath tube provided an oxygen-free environment. A TC was placed at the side of the metal sheath tube for the reference temperature, and the measurement point was matched to the location of the diamond thermistor. The thermistor was inserted into the box furnace by putting the sheath tube halfway through the window of the furnace chamber, and the two wires from the diamond thermistor were connected to the source-meter at the outside of the furnace chamber. A 2-wire measurement method was used for the resistance measurement, and 1 V was applied between the wires to obtain current readings. The source-meter and TC were controlled by LABVIEW measuring 6 resistance data per second and temperature data every 0.8 seconds, respectively.

To measure the resistance with respect to the temperature, the furnace was first heated up to a maximum temperature of interest, followed by insertion of instruments in the furnace chamber. After starting the measurement, the furnace was turned off to slowly decrease the temperature. Fig. 5 is the resistance data of CVD and HPHT diamond thermistor with respect to the temperature of the reference TC. The measured temperature ranges were 115 - 880 °C for the CVD diamond and 145 - 850 °C for the HPHT diamond. The green dots are the resistance data of CVD diamond thermistor and the blue dots are resistance data of HPHT diamond thermistor. Both diamond thermistors showed exponential resistance decrement to the temperature increment, and the resistance of HPHT diamond decreased faster than CVD diamond. This is because the doping concentrations of the dopants are higher in HPHT diamond than CVD diamond. The dopants make additional energy levels at the bandgap of the diamond which produces additional carriers that reduce resistance [38]. The resistance of CVD and HPHT diamonds exceeded 5 GΩ and started to fluctuate severely when the temperature was below 330 °C and 210 °C, respectively. The red lines on top of both resistance

data are derived from the Steinhart-Hart equation. We divided the temperature range into several sections and used 3 data points within that temperature range to extract the closest fitting curve. For example, the first temperature range for CVD diamond thermistor is 320-360 °C using 3 data points at 350 °C, 355 °C, and 360 °C, and the last temperature range is 510-900 °C using 3 data points at 536 °C, 610 °C, and 800 °C. Similar method was applied to HPHT diamond thermistor starting from 210 °C to 900 °C. Suitable temperature range can be selected depending on the temperature of interest to convert the resistance data into temperature data, or a new Steinhart-Hart curve can be derived using 3 data points near at the desired temperature. The CVD diamond thermistor shows potential to operate higher than the maximum temperature measured in this test because its resistance value is around 380 kΩ at 880 °C. This is 2000 times higher than that of the HPHT diamond thermistor, that is 190 Ω at 850 °C. The resistance is expected to decrease exponentially more than that of HPHT diamond thermistor as the temperature increases above 880 °C. The resistances of CAR at the diamond region were also measured and plotted in a pink dashed line in Fig. 5 to check the leakage current through the crushable alumina. A separate sheath tube device was fabricated with the same materials and method, but without the diamond thermistor, to measure the resistance of CAR. The resistance was higher than the resistance of CVD and HPHT diamonds, suggesting that the currents were flown through the diamond instead of through the surrounding insulation material. The maximum temperature limit of the sheath tube design was around 921 °C due to the silver paste. The resistance of the silver paste was suddenly increased to the MΩ range after 921 °C. Further increment of the temperature contaminated the surface of diamond permanently with silver paste residues causing an electrical short.

The sensitivity of CVD diamond thermistor is lower than the HPHT diamond thermistor because of the smaller decrement of the resistance. Comparing the temperature coefficient of both thermistors support this that can be expressed in:

$$\alpha = \frac{dR}{dT} / R. \tag{2}$$

where α is the temperature coefficient, T is temperature, and R is resistance. The temperature coefficients of HPHT and CVD diamond thermistors are shown in fig. 6. The blue line is the HPHT diamond thermistor, and the green line is the CVD diamond thermistor. The HPHT diamond thermistor had higher temperature coefficients as described earlier. Both thermistors show the temperature coefficient higher than 0.01 K^{-1} throughout the temperature ranges that are higher than other types of temperature sensors such as resistance temperature detectors [39].

The stability of the sheath tube design under abrupt temperature change was tested with CVD diamond thermistor by repeatedly taking the thermistor tube in and out of the heated furnace. The thermistor was heated up to 880 °C when the sheath tube was inside the furnace and cooled at room temperature when it was pulled out. Fig. 7 shows a diamond thermistor tube taken out from the window of the furnace after

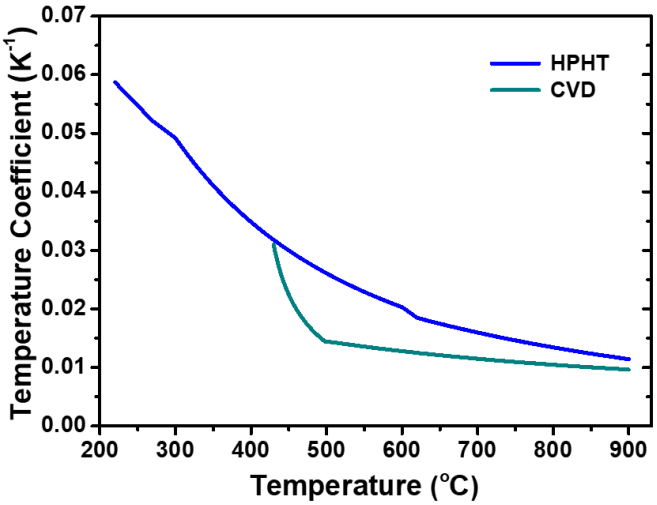

Fig. 6. Temperature coefficients of HPHT and CVD diamond thermistors.

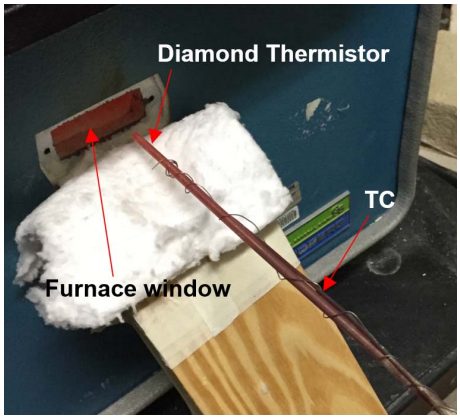

Fig. 7. Image of diamond thermistor tube taken out from the furnace for the 880 °C heating cycle test.

it was heated up to 880 °C. There was no deformation or damage to the metal tube from the outside except for the red heat. The results of 880 °C cycling test with CVD diamond thermistor is plotted in Fig. 8. The blue dots are the resistance data of the thermistor and the orange dots are the temperature data from the reference TC. Starting from the outside of the furnace, the thermistor tube was put into the furnace for 8 minutes and pulled out for 3 minutes to cool. The test was repeated for 2 cycles in a similar way. The resistance of CVD diamond decreased to 380 kΩ when the thermistor was stabilized inside the furnace and increased back to high resistance oscillating between 10 GΩ and 11 GΩ when pulled out. Despite the large temperature variance, the swaged sheath tube successfully prevented the silver paste from separating from the diamond contact pads due to the thermal expansion differences, and the electrical connection to the diamond was maintained during the cycling test.

The long-term stability test was studied under various temperatures with the CVD diamond thermistor in metal sheath design. The resistance was measured every 0.8 seconds for 10 hours at each test temperatures: 500 °C, 600 °C, 700 °C,

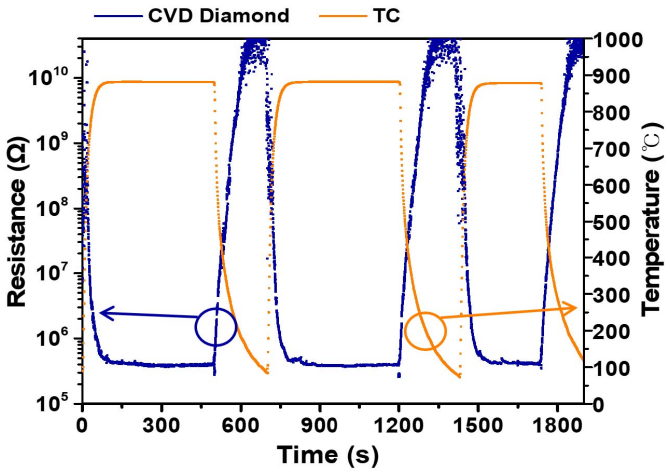

Fig. 8. The stability test results of electrical connection to the diamond under 880 °C heating cycle test with CVD diamond thermistor with a metal sheath tube design.

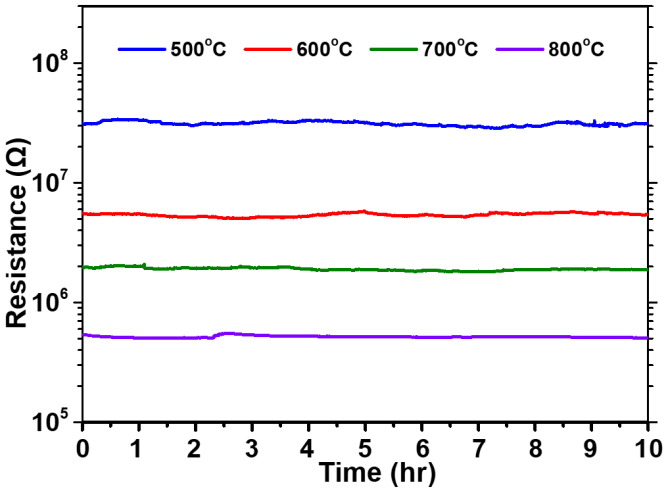

Fig. 9. Resistance results of long-term stability test at different temperatures.

and 800 °C. A TC was inserted with the CVD diamond thermistor to monitor the temperature inside the furnace where the thermistor is located. The temperature of the furnace was stable at the set temperature fluctuating less than 0.1 °C during the experiment according to the TC. The test results under 4 temperatures are plotted in Fig. 9. The resistance of the thermistor changed to the levels shown in Fig. 5 when the test temperature is changed and minor fluctuations were observed for each of the cases during the measurement.

The average and standard deviation analysis results are shown in Table 1. Average resistance and the standard deviation of resistance are calculated using all of the resistance data for each of the test temperature. The coefficient of variation is calculated by dividing the standard deviation of resistance by average resistance and converted into percentages to compare the results and shown. Finally, the standard deviation of temperature is the standard deviation of converted temperature data using the Steinhart-Hart equation. The average resistance and the standard deviation of the resistance became

TABLE I
RESULTS OF THE LONG-TERM STABILITY TEST

Temperature (□)	Average Resistance (MΩ)	Standard Deviation of Resistance (kΩ)	Coefficient of Variation (%)*	Standard Deviation of Temperature (□)
500	31.3178	1250.40	3.992	3.075
600	5.40180	179.017	3.314	2.841
700	1.90202	53.6899	2.823	2.321
800	0.516796	9.4761	1.834	1.746

* Standard Deviation of Resistance as a percent of average resistance.

lower as the test temperature increases due to the nature of the thermistor. The percentage of coefficient of variation became smaller as the test temperature increased meaning the fluctuation of the resistance is decreasing. This is because of less influence of noises since the measured currents are increasing due to the decrement of the diamond's resistance as the test temperature increases. Similarly, the standard deviation of temperature became smaller at a higher temperature. The overall long-term stability of the diamond thermistor with metal sheath tube design suggests stable operations without abrupt errors. The sheath tube protected the diamond from oxygen and maintained a stable electrical connection between the silver paste and the contact pad of the diamond.

III. CONCLUSIONS

The diamond thermistor was fabricated with HPHT and CVD diamonds for high temperature sensing applications. The HPHT diamond thermistor was tested with the alumina tube design with connection wires fixed to the thermistor contact pads by silver paste. The resistance was measured up to 700 °C and the resistance results of the HPHT diamond were well-fitted to the curve of the Steinhart-Hart equation. However, continual measurement at higher temperatures failed due to the separation of connection wires from the contact pad caused by the thermal expansion differences of the diamond and silver paste. To overcome the issue, a metal sheath tube design was introduced to reinforce the adhesion by swaging the metal tube, which adds a compressive force to maintain contact with the diamond thermistor. The operation of HPHT and CVD diamond thermistors with the metal sheath tube design was tested up to 850 °C and 880 °C, respectively, showing typical resistance results of the diamond thermistor with respect to temperature. The HPHT diamond thermistor showed higher temperature sensitivity because the change of the resistance was larger than the CVD diamond. The CVD diamond thermistor showed the potential to operate at a higher temperature because the resistance level at 880 °C was still large enough to decrease exponentially.

Experiments were also conducted to test thermistor stability under abrupt temperature changes and under various temperatures for 10 hours with the metal sheath tube design using the CVD diamond thermistor. The resistance of the thermistor showed consistent results during the cycling heating test at

880 °C showing the swaged sheath tube successfully held the wire connection to the diamond contact pads. During the long-term stability test, the deviations in resistance became smaller as the test temperature increased. The diamond thermistor with the metal sheath tube design showed stable operation without large resistance variations or sudden drifts. We expect that the operating temperature range of the diamond thermistor can be extended to higher ranges with the metal sheath tube design if the wire connecting method is replaced by other approaches that resist a higher temperature environment such as bonding Mo wires directly to the diamond surface with diffusion bonding process.

ACKNOWLEDGMENT

The authors would like to thank Ms. S. Schupner, DOE, and Dr. C. Jensen, INL for the supports of our works.

REFERENCES

[1] A. Feteira, "Negative temperature coefficient resistance (NTCR) ceramic thermistors: An industrial perspective," *J. Amer. Ceram. Soc.*, vol. 92, no. 5, pp. 967–983, May 2009.
[2] C. C. Wang, S. A. Akbar, and M. J. Madou, "Ceramic based resistive sensors," *J. Electroceram.*, vol. 2, pp. 273–282, Dec. 1998.
[3] G. B. Rodgers and F. A. Raal, "Semiconducting diamonds as thermistors," *Rev. Sci. Instrum.*, vol. 31, no. 6, pp. 663–664, 1960.
[4] P. W. May, "Diamond thin films: A 21st-century material," *Philos. Trans. Math. Phys. Eng. Sci.*, vol. 358, pp. 473–495, Jan. 2000.
[5] T. Irifune, A. Kurio, S. Sakamoto, T. Inoue, and H. Sumiya, "Ultrahard polycrystalline diamond from graphite," *Nature*, vol. 421, pp. 599–600, Feb. 2003.
[6] V. Blank, M. Popov, G. Pivovarov, N. Lvova, K. Gogolinsky, and V. Reshetov, "Ultrahard and superhard phases of fullerite C_{60}: Comparison with diamond on hardness and wear," *Diamond Rel. Mater.*, vol. 7, pp. 427–431, Feb. 1998.
[7] T. R. Anthony *et al.*, "Thermal diffusivity of isotopically enriched ^{12}C diamond," *Phys. Rev. B*, vol. 42, pp. 1104–1111, Jul. 1990.
[8] L. Wei, P. K. Kuo, R. L. Thomas, T. R. Anthony, and W. F. Banholzer, "Thermal conductivity of isotopically modified single crystal diamond," *Phys. Rev. Lett.*, vol. 70, pp. 3764–3767, Jun. 1993.
[9] J. Walker, "Optical absorption and luminescence in diamond," *Rep. Prog. Phys.*, vol. 42, p. 1605–1659, Oct. 1979.
[10] M. N. Yoder, "Wide bandgap semiconductor materials and devices," *IEEE Trans. Electron Devices*, vol. 43, no. 10, pp. 1633–1636, Oct. 1996.
[11] V. S. Bormashov *et al.*, "Fast-response thermistors made of synthetic single-crystal diamonds," *Instrum. Exp. Techn.*, vol. 52, pp. 738–742, Sep. 2009.
[12] J. F. H. Custers, "Semiconductivity of a type IIbdiamond," *Nature*, vol. 176, pp. 173–174, Jul. 1955.
[13] I. G. Austin and R. Wolfe, "Electrical and optical properties of a semiconducting diamond," *Proc. Phys. Soc. Sect. B*, vol. 69, no. 3, pp. 329–338, 1956.
[14] P. T. Wedepohl, "Electrical and optical properties of type IIb diamonds," *Proc. Phys. Soc. Sect. B*, vol. 70, pp. 177–185, Feb. 1957.
[15] F. P. Bundy, H. T. Hall, H. M. Strong, and R. H. Wentorf, "Man-made diamonds," *Nature*, vol. 176, pp. 51–55, Jul. 1955.
[16] H. P. Bovenkerk, F. P. Bundy, H. T. Hall, H. M. Strong, and R. H. Wentorf, "Preparation of diamond," *Nature*, vol. 184, pp. 1094–1098, Oct. 1959.
[17] H. Sumiya and S. Satoh, "High-pressure synthesis of high-purity diamond crystal," *Diamond Rel. Mater.*, vol. 5, pp. 1359–1365, Nov. 1996.
[18] H. M. Strong and R. M. Chrenko, "Diamond growth rates and physical properties of laboratory-made diamond," *J. Physical Chem.*, vol. 75, no. 12, pp. 1838–1843, 1971.
[19] M. Schwander and K. Partes, "A review of diamond synthesis by CVD processes," *Diamond Rel. Mater.*, vol. 20, pp. 1287–1301, Oct. 2011.
[20] M. N. R. Ashfold, P. W. May, C. A. Rego, and N. M. Everitt, "Thin film diamond by chemical vapour deposition methods," *Chem. Soc. Rev.*, vol. 23, pp. 21–30, Feb. 1994.
[21] B. V. Spitsyn, L. L. Bouilov, and B. V. Derjaguin, "Vapor growth of diamond on diamond and other surfaces," *J. Crystal Growth*, vol. 52, pp. 219–226, Apr. 1981.
[22] S. Matsumoto, Y. Sato, M. Tsutsumi, and N. Setaka, "Growth of diamond particles from methane-hydrogen gas," *J. Mater. Sci.*, vol. 17, pp. 3106–3112, Nov. 1982.
[23] W. Zhu, B. R. Stoner, B. E. Williams, and J. T. Glass, "Growth and characterization of diamond films on nondiamond substrates for electronic applications," *Proc. IEEE*, vol. 79, no. 5, pp. 621–646, May 1991.
[24] N. Setaka, "A few problem in the vapor deposition of diamond," *MRS Online Proc. Library Arch.*, vol. 152, p. 3, 1989.
[25] J. P. Bade *et al.*, "Fabrication of diamond thin-film thermistors for high-temperature applications," *Diamond Rel. Mater.*, vol. 2, pp. 816–819, Apr. 1993.
[26] K. Miyata, K. Saito, K. Nishimura, and K. Kobashi, "Fabrication and characterization of diamond film thermistors," *Rev. Sci. Instrum.*, vol. 65, pp. 3799–3803, Dec. 1994.
[27] K. L. Moazed, J. R. Zeidler, and M. J. Taylor, "A thermally activated solid state reaction process for fabricating ohmic contacts to semiconducting diamond," *J. Appl. Phys.*, vol. 68, pp. 2246–2254, Sep. 1990.
[28] M. Roser, C. A. Hewett, K. L. Moazed, and J. R. Zeidler, "High-temperature reliability of refractory-metal ohmic contacts to diamond," *J. Electrochem. Soc.*, vol. 139, pp. 2001–2004, Jul. 1992.
[29] J. Nakanishi, A. Otsuki, T. Oku, and O. Ishiwata, "Formation of ohmic contacts to p-type diamond using carbide forming metals," *J. Appl. Phys.*, vol. 76, pp. 2293–2298, Aug. 1994.
[30] P. John, N. Polwart, C. E. Troupe, and J. I. B. Wilson, "The oxidation of (100) textured diamond," *Diamond Rel. Mater.*, vol. 11, pp. 861–866, Mar./Jun. 2002.
[31] J.-C. Pu, S.-F. Wang, and J. C. Sung, "High-temperature oxidation behaviors of CVD diamond films," *Appl. Surf. Sci.*, vol. 256, pp. 668–673, Nov. 2009.
[32] D. Schryer, E. A. Gulbransen, K. F. Andrew, and F. A. Brassart, "Oxidation of Molybdenum 550-Degrees-C to 1700-Degrees-C," *J. Electrochem. Soc.*, vol. 111, pp. 757–762, Jan. 1963.
[33] H. A. Hoff *et al.*, "Ohmic contacts to semiconducting diamond using a Ti/Pt/Au trilayer metallization scheme," *Diamond Rel. Mater.*, vol. 5, pp. 1450–1456, Dec. 1996.
[34] J. G. Ran, C. Q. Zheng, J. Ren, and S. M. Hong, "Properties and texture of B-doped diamond films as thermal sensor," *Diamond Rel. Mater.*, vol. 2, pp. 793–796, Apr. 1993.
[35] G. S. Yang, D. M. Aslam, M. White, and J. J. McGrath, "The characterization of single structure diamond heater and temperature sensor," *Diamond Rel. Mater.*, vol. 6, pp. 394–397, Mar. 1997.
[36] J. S. Steinhart and S. R. Hart, "Calibration curves for thermistors," *Deep Sea Res. Oceanographic Abstr.*, vol. 15, pp. 497–503, Aug. 1968.
[37] J. L. Rempe, D. L. Knudson, K. G. Condie, and S. C. Wilkins, "Thermocouples for high-temperature in-pile testing," *Nucl. Technol.*, vol. 156, pp. 320–331, Dec. 2006.
[38] J. A. Becker, C. B. Green, and G. L. Pearson, "Properties and uses of thermistors—Thermally sensitive resistors," *Trans. Amer. Inst. Elect. Eng.*, vol. 65, no. 11, pp. 711–725, Nov. 1947.
[39] B. Baker, "Temperature sensing technologies," Microchip Technology Inc, Chandler, AZ, USA, Tech. Rep. AN679, 1998.

Tong J. Kim was born in Beaumont, TX, USA, in 1984. He received the B.S. degree in electrical engineering from Yonsei University, Seoul, South Korea, in 2012, and the M.S. and Ph.D. degrees in electrical engineering from the University of Wisconsin–Madison, Madison, WI, USA, in 2015 and 2018, respectively.

He is currently a Post-Doctoral Associate with the National High Magnetic Field Laboratory, Tallahassee, FL, USA. His research interests include developing high-power supply control system for DC field magnets and superconductor magnets.

Kurt L. Davis is a Principal Researcher with the High Temperature Test Laboratory, Idaho National Laboratory, Idaho Falls, ID, USA. He was the NASA product improvement Team Leader for the space shuttle, and currently the Principle Investigator representing the Idaho National Laboratory on the Integrated Research Project for advanced instrumentation for transient reactor testing. His research interest is the development and fabrication of new sensors, X-ray system design and operation, high-temperature testing, nuclear material handling, and thermal modeling.

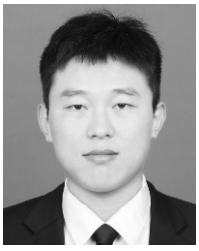

Yunpeng Liu received the B.S. and Ph.D. degrees in applied physics from the Nanjing University of Aeronautics and Astronautics (NUAA) in 2009 and 2014, respectively.

He is currently an Associate Professor with the Department of Nuclear Science and Engineering, NUAA. He published more than 20 papers related to his research and holds 11 Chinese patents. His research interests are the applications of Monte Carlo method in particle transport, the design and preparation of new nuclear battery, and space X-ray communication technology.

John R. (Jack) Bredemann was born in Kansas, MO, USA, in 1991. He received the B.S. degree in physics from the University of Dallas at Irving, Irving, TX, USA, in 2014, and the M.S. degree from the University of Wisconsin–Madison, Madison, WI, USA, in 2018.

He is currently a Computer Support Representative for Epic Systems, Verona, WI, USA.

Zhenqiang (Jack) Ma (S'98–M'01–SM'12–F'18) received the B.S. degree in applied physics and the B.E. degree in electrical engineering from Tsinghua University, Beijing, China, in 1991, the M.S. degree in nuclear science and the M.S.E. degree in electrical engineering from the University of Michigan, Ann Arbor, in 1997, and the Ph.D. degree in electrical engineering from the University of Michigan in 2001.

From 2001 to 2002, he was a member of the R&D Team at Conexant Systems and later its spin-off, Jazz Semiconductor (now TowerJazz), in Newport Beach, CA, USA. In 2002, he left Jazz to join the faculty of the University of Wisconsin–Madison as an Assistant Professor with the Department of Electrical and Computer Engineering. He is currently a Lynn H. Matthias Professor of Engineering and a Vilas Distinguished Achievement Professor with affiliated appointments in four other departments and research institutes in engineering and medical school. His current interdisciplinary research covers electrical engineering, materials science and engineering, and biomedical engineering. He has authored or coauthored about 500 technical papers and book chapters related to his research. He holds several dozens of U.S., foreign, and international patents. His present research interests focus on the materials, physics and device applications of lattice-mismatched 3D-semiconductor heterostructures, microwave flexible electronics, semiconductor nanomembrane-based sensors, and bioelectronics. He is a Fellow of the AAAS, AIMBE, APS, NAI, and OSA.

Mark Anderson received the B.S. degree in physics from the University of Wisconsin, River Falls, WI, USA, in 1993, and the Ph.D. degree in nuclear engineering from the University of Wisconsin, Madison, WI, USA, in 1998.

He is a Professor with the Mechanical Department and the Director of the University of Wisconsin's Thermal Hydraulic Laboratory. He was awarded five patents and has published over 100 journal publications. He has expertise in high-temperature sensor and thermal designs for energy-based systems, and has extensive experience in reactor thermal hydraulics.

Michael L. Corradini received the B.S. degree in mechanical engineering from Marquette University, Milwaukee, WI, USA, in 1975, and the M.S. and Ph.D. degrees in nuclear engineering from the Massachusetts Institute of Technology, MA, USA, in 1976 and 1978, respectively.

He is an Emeritus Professor of Nuclear Engineering with the University of Wisconsin–Madison. He has published widely in areas related to transport phenomena in multiphase systems. He was elected to the National Academy of Engineering in 1998. From 2004 to 2008, he was a Board Member of the INPO National Accreditation Board for Nuclear Training. In 2006, he was appointed to the NRC Advisory Committee on Reactor Safeguards. Most recently, he was appointed as the Chair of the Scientific Advisory Committee, French Atomic Energy Agency. He began and served as the Director of the Wisconsin Energy Institute.